NASA/TM—2007-214801

Catalytic Ignition and Upstream Reaction Propagation in a Platinum Tube

P.M. Struk and D.L. Dietrich
Glenn Research Center, Cleveland, Ohio

B.P. Mellish and F.J. Miller
National Center for Space Exploration Research, Cleveland, Ohio

J.S. T'ien
Case Western Reserve University, Cleveland, Ohio

June 2007

NASA STI Program . . . in Profile

Since its founding, NASA has been dedicated to the advancement of aeronautics and space science. The NASA Scientific and Technical Information (STI) program plays a key part in helping NASA maintain this important role.

The NASA STI Program operates under the auspices of the Agency Chief Information Officer. It collects, organizes, provides for archiving, and disseminates NASA's STI. The NASA STI program provides access to the NASA Aeronautics and Space Database and its public interface, the NASA Technical Reports Server, thus providing one of the largest collections of aeronautical and space science STI in the world. Results are published in both non-NASA channels and by NASA in the NASA STI Report Series, which includes the following report types:

- TECHNICAL PUBLICATION. Reports of completed research or a major significant phase of research that present the results of NASA programs and include extensive data or theoretical analysis. Includes compilations of significant scientific and technical data and information deemed to be of continuing reference value. NASA counterpart of peer-reviewed formal professional papers but has less stringent limitations on manuscript length and extent of graphic presentations.

- TECHNICAL MEMORANDUM. Scientific and technical findings that are preliminary or of specialized interest, e.g., quick release reports, working papers, and bibliographies that contain minimal annotation. Does not contain extensive analysis.

- CONTRACTOR REPORT. Scientific and technical findings by NASA-sponsored contractors and grantees.

- CONFERENCE PUBLICATION. Collected papers from scientific and technical conferences, symposia, seminars, or other meetings sponsored or cosponsored by NASA.

- SPECIAL PUBLICATION. Scientific, technical, or historical information from NASA programs, projects, and missions, often concerned with subjects having substantial public interest.

- TECHNICAL TRANSLATION. English-language translations of foreign scientific and technical material pertinent to NASA's mission.

Specialized services also include creating custom thesauri, building customized databases, organizing and publishing research results.

For more information about the NASA STI program, see the following:

- Access the NASA STI program home page at *http://www.sti.nasa.gov*

- E-mail your question via the Internet to *help@sti.nasa.gov*

- Fax your question to the NASA STI Help Desk at 301–621–0134

- Telephone the NASA STI Help Desk at 301–621–0390

- Write to:
  NASA Center for AeroSpace Information (CASI)
  7115 Standard Drive
  Hanover, MD 21076–1320

NASA/TM—2007-214801

Catalytic Ignition and Upstream Reaction Propagation in a Platinum Tube

P.M. Struk and D.L. Dietrich
Glenn Research Center, Cleveland, Ohio

B.P. Mellish and F.J. Miller
National Center for Space Exploration Research, Cleveland, Ohio

J.S. T'ien
Case Western Reserve University, Cleveland, Ohio

Prepared for the
2006 Technical Meeting on Combustion Fundamentals and Applications
sponsored by The Combustion Institute
Cleveland, Ohio, May 21–23, 2006

National Aeronautics and
Space Administration

Glenn Research Center
Cleveland, Ohio 44135

June 2007

Acknowledgments

The authors gratefully acknowledge support from NASA to the National Center for Space Exploration Research (NCSER) and Case Western Reserve University (CWRU) under Cooperative Agreement NNC04AA29A.

Level of Review: This material has been technically reviewed by technical management.

Available from

NASA Center for Aerospace Information
7115 Standard Drive
Hanover, MD 21076–1320

National Technical Information Service
5285 Port Royal Road
Springfield, VA 22161

Available electronically at http://gltrs.grc.nasa.gov

Catalytic Ignition and Upstream Reaction Propagation in a Platinum Tube

P.M. Struk and D.L. Dietrich
National Aeronautics and Space Administration
Glenn Research Center
Cleveland, Ohio 44135

B.P. Mellish and F.J. Miller
National Center for Space Exploration Research
Cleveland, Ohio 44135

J.S. T'ien
Case Western Reserve University
Cleveland, Ohio 44106

Abstract

A challenge for catalytic combustion in monolithic reactors at elevated temperatures is the start-up or "light-off" from a cold initial condition. In this work, we demonstrate a concept called "back-end" catalytic ignition that potentially can be utilized in the light-off of catalytic monoliths. An external downstream flame or Joule heating raises the temperature of a small portion of the catalyst near the outlet initiating a localized catalytic reaction that propagates upstream heating the entire channel. This work uses a transient numerical model to demonstrate "back-end" ignition within a single channel which can characterize the overall performance of a monolith. The paper presents comparisons to an experiment using a single non-adiabatic channel but the concept can be extended to the adiabatic monolith case.

In the model, the time scales associated with solid heat-up are typically several orders of magnitude larger than the gas-phase and chemical kinetic time-scales. Therefore, the model assumes a quasi-steady gas-phase with respect to a transient solid. The gas phase is one-dimensional. Appropriate correlations, however, account for heat and mass transfer in a direction perpendicular to the flow. The thermally-thin solid includes axial conduction. The gas phase, however, does not include axial conduction due to the high Peclet number flows. The model includes both detailed gas-phase and catalytic surface reactions. The experiment utilizes a pure platinum circular channel oriented horizontally though which a CO/O_2 mixture (equivalence ratios ranging from 0.6 to 0.9) flows at 2 m/s.

Introduction

Catalytic combustion has long been recognized for its potential to reduce temperatures of power generation devices in both large and small scale applications. Such power generation devices often use a monolith structure coated with a catalyst through which passes a pre-mixed combustible gas mixture [1,2]. The monolith (catalyst) must be at an elevated temperature to initiate a reaction. One challenge for such devices is the start-up from a cold initial condition. We propose a new concept for the start-up of a catalytic monolith utilizing a "back-end" ignition scheme. In this concept, a downstream flame or Joule heating raise the temperature of a small portion of the solid near the outlet of the catalyst section initiating a localized catalytic reaction. The reaction releases sufficient heat (even after removal of the external heat source) and the reaction front begins to propagate upstream via solid conduction ultimately preheating the entire monolith. In this work, we demonstrate the feasibility of "back-end" catalytic ignition using a transient catalytic combustor model and compare the results to a laboratory experiment. We calculate the propagation velocity of the catalytic reaction front for a range of equivalence ratios, ϕ, using carbon monoxide in pure oxygen. The experiment utilizes a single horizontal platinum tube. The tube is non-adiabatic but the concept can be extended to the adiabatic (monolith) case.

Specific Objectives

(1) Demonstrate "back-end" ignition for a catalytic channel using a transient model with CO/O_2.

(2) Compare model predictions of catalytic propagation velocity to experimental data.

(3) Show the effect of ϕ on catalytic reaction front propagation speed for a fixed inlet velocity.

Model Description

Overview

The catalytic reactor is a single tube or channel which, for a large scale reactor, represents a single channel in a monolith. The tube is either made of a catalytically active material (platinum in this work) or a solid substrate coated with a catalytic material. A premixed gas of fuel, oxidizer, and

optional inert (K_g total gas species) enters the channel with a prescribed velocity. The combustion process considers both detailed gas phase and surface reactions. There is negligible pressure drop along the channel and the gas is ideal. The transient combustor time-lag is from the thermal inertia of the solid [3]. The gas-phase model (eqs. (1) to (4)) is quasi-steady relative to the transient solid (eqs. (5) to (7)) owing to the significantly longer heat-up times of the solid (~sec) compared with the residence times of the gas in the channel (~msec). In the gas-phase equations, heat and mass diffusion in the axial direction are neglected because the Peclet number based on typical gas velocities is much greater than unity.

Bulk temperatures, assuming no lateral gradients (i.e., perpendicular to the flow), describe the solid (T_s) and gas (T) along the channel. The model considers heat transfer perpendicular to the flow using an axially varying heat transfer coefficient (h_T) from a Nusselt number correlation for developing flow in an isothermal circular tube. In eq. (3), if the reaction rate of species k due to catalytic reactions, $\dot{s}_k$, is greater than 0 (gas-species k desorbing from the surface) then the enthalpy of species k (h_k) is evaluated at the surface temperature ($T' = T_S$). For $\dot{s}_k < 0$ (gas-species k adsorbing to the surface), h_k is evaluated at the bulk gas temperature ($T' = T$).

There are two values of gas-phase species mass-fraction, a bulk flow value (Y_k) and a value adjacent to the catalytic surface but still in the gas-phase (Y_{kW}). Lateral mass transfer coefficients come from the heat transfer coefficients using the analogy of heat and mass transfer [4]. The value of Y_{kW} comes from a balance between lateral mass transfer and the adsorption or desorption of species on the catalytic surface (eq. (5)). Transport properties are calculated using the bulk temperature and mass fraction at each axial location.

The transient solid-phase energy equation (eq. (6)) includes heat transfer to and from the gas inside the tube, external heat transfer to the surroundings, heat generation terms due to catalytic reactions and Joule heating, and axial heat conduction. The external heat loss due to natural convection (term 3) and radiation (term 4) allows modeling of a single catalytic channel for comparison to the experiments. The external heat loss from natural convection comes from correlations of Churchill and Chu [5]. For a single (central) channel of a monolith reactor, the external heat loss terms are set to zero. The enthalpy of absorbing and desorbing gas species (term 5) are evaluated just as described previously for the gas-phase. Because the solid is thermally thin, the surface catalytic reactions (those involving surface species only) are modeled as surface heat generation (term 6) in the solid. A prescribed volumetric heat generation (term 7) simulates Joule or external heating of the solid. Term 8 represents the axial heat transfer due to conduction. The solid density, ρ_S; heat capacity, C_S; and thermal conductivity, λ; are all constant in the model. A complete nomenclature section can be found in Struk et al. [6].

The model of the catalytic reactions along the inner portion of the channel wall accounts for varying surface coverage of adsorbed species (eq. (6)). There are K_S total surface species including vacant surface sites. The model assumes that the number of active surface sites, Γ (= 2.7063×10^{-9} mol/m^2 for platinum), is constant (eq. (7)).

Chemistry

The gas mixtures for this study included only carbon monoxide (CO) and pure oxygen (O_2) with no hydrogen containing species or inert. The model tracks the following species: O, CO, O_2, CO_2, Pt(s), CO(s), CO_2(s), C(s), and O(s). The "(s)" denotes species adsorbed to the surface while the symbol Pt(s) denotes vacant sites of the platinum surface. The gas-phase utilizes a subset, steps 8, 21, and 23 (n_g = 3), of the mechanism proposed by Davis et al. [7,8]—the remaining reactions deal with hydrogen chemistry and are neglected. The heterogeneous reactions, which account for species adsorption, surface reactions, and desorption, come from a subset of a CH_4/O_2 on platinum mechanism proposed by Deutschmann et al. [9,10] namely steps 4, 5, 6, 14, 15, 16, 17, 22, and 23 (n_s = 9). The gas-phase, $\dot{\omega}_k$, and surface, $\dot{s}_k$, reactions are evaluated using eqs. (8) to (10) where q_i is the rate of the i^{th} reaction and ν is the stoichiometric coefficient.

Initial and Boundary Conditions

The inlet boundary conditions for the gas-phase equations (eqs. (1) to (4)) are a temperature of 300 K, a velocity of 2 m/s, a pressure of 1 atm, and a fuel equivalence ratio ranging from ϕ = 0.6 to 0.9 (no diluent). The solid energy equation (eq. (6)) requires 2 boundary conditions due to the axial conduction term. The inlet boundary is at 300 K to simulate the large heat sink (fitting) present in the experiment. The outlet of the solid channel is adiabatic. The transient equations (eqs. (6) to (7)) require initial conditions for surface temperature and site fraction distribution along the length of the channel. The initial surface temperature is 300 K while all surface sites contain O (i.e., surface site fraction $Z_{O(S)}$ = 1). The initial condition for the remaining unknown, Y_{kW}, comes from an algebraic solution of eq. (5).

The ignition scheme mimics the experiment with heat input from a nearby flame at the tube outlet. The generation term, $\dot{q}_{gen}$, is set at 2.5 W for the last (downstream) 10% of the tube for a set time (either 2 or 3 sec). For these tests, the length of the tube is 3.5 cm.

Gas Phase Equations

Equation of State:

$$\rho = \frac{P}{\left(R_U / \overline{W}\right) T} \tag{1}$$

Overall mass-conservation:

$$\dot{m} = \rho u A \,(\text{constant}) \tag{2}$$

Energy conservation:

$$\rho u A C_P \frac{\partial T}{\partial x} + A\sum_{k=1}^{Kg} \dot{\omega}_k W_k h_k + S\sum_{k=1}^{Kg} \dot{s}_k W_k \left[h_k(T) - h_k(T')\right] + h_T S\left[T - T_S\right] = 0$$

$$T' = \begin{cases} T \text{ if } \dot{s}_K \le 0 \\ T_S \text{ if } \dot{s}_K > 0 \end{cases} \tag{3}$$

Species conservation for species *k*:

$$\rho u A \frac{\partial Y_k}{\partial x} = \dot{s}_k W_k S + \dot{\omega}_k W_k A \tag{4}$$

Surface Equations

Flux-matching at the surface:

$$\rho h_{Dk}\left(Y_k - Y_{kW}\right) = -\dot{s}_k W_k \tag{5}$$

Solid Phase Equations

Energy conservation:

$$\rho_S C_S A_S \frac{\partial T_S}{\partial t} = h_T S\left(T - T_S\right) - h_O S_O\left(T_S - T_\infty\right) - \varepsilon\sigma S_O\left(T_S^4 - T_\infty^4\right) - S\sum_{k=1}^{K_g} \dot{s}_k W_k h_k(T') + S\sum_{k=1}^{K_S} \dot{s}_k W_k h_k(T_S) + \dot{q}_{gen} A_S + \frac{\partial}{\partial x}\left(kA_S \frac{\partial T_S}{\partial x}\right) \tag{6}$$

Rate of change of surface site fractions:

$$\frac{\partial Z_k}{\partial t} = \frac{1}{\Gamma}\dot{s}_k \quad (k = 1 \ldots K_S) \tag{7}$$

Chemistry Expressions

$$\dot{\omega}_k = \sum_{i=1}^{n_g} \nu_{ki} q_i \tag{8}$$

$$\dot{s}_k = \sum_{i=1}^{n_S} \nu_{ki} q_i \tag{9}$$

$$q_i = k_{fi}\prod_{k=1}^{K}\left[X_k\right]^{\nu'_{ki}} - k_{ri}\prod_{k=1}^{K}\left[X_k\right]^{\nu''_{ki}} \tag{10}$$

Thermophysical Properties and Geometric Parameters

The thermophysical properties and geometric parameters of the catalytic tube used in model are shown in table 1. The property values come from Incropera and DeWitt [4]. The density and specific heat of the solid do not vary significantly with temperature. The thermal conductivity varies only ~10% across the temperature range from 300 to 1200 K. Consequently, a constant thermal conductivity is assumed (corresponding to the value at 600 K). The emissivity corresponds to the value at the approximate maximum temperature (~1200 K) predicted by the model. The geometric values are chosen to match the experimental setup.

TABLE 1.—THERMO PHYSICAL AND GEOMETRIC PARAMETERS

Material	Platinum
ρ, Density @ 300 K (kg/m^3)	21450
C_p, Heat capacity @ 300 K (J/kg/K)	133
λ, Thermal conductivity @ 600 K (W/m/K)	73
ε, Emissivity @1200 K	0.15
Cross-sectional Geometry	Circular
D, Inner diameter (mm)	0.8
D_O, Outer diameter (mm)	1.0
L, Channel length (mm)	35.0

Solution Procedure

In general, the dependent variables (T, T_S, Y_k, Y_{kW}, and Z_k) as well as all the property values, transport coefficients, and reaction rate terms are functions of axial position and time. Equations (1) and (2) substitute directly into the remaining equations. Thus, eqs. (3) to (7) form a system of partial differential equations (PDE) for the gas, surface, and solid.

Equations (5) to (7) represent the solid-phase and surface. Both eqs. (5) (surface flux balance) and (6) (solid-phase energy balance) directly couple to the gas-phase variables Y_k and T, respectively. Equation (6) is a PDE which transforms into an ODE via the "method of lines" by dividing the solid into a number of small finite volumes. Separate conservation equations (i.e., eqs. (5) to (7)) can be written for each volume (175 in this case) and adjacent surface thus forming a large system (~2000) of ordinary differential-algebraic equations (DAE).

Since the gas-phase is quasi-steady, it responds instantly to changes on the solid and surface. Thus, in principle, the gas-phase must be solved simultaneously with the changing solid

phase and surface variables. In order to capture homogeneous ignition, however, a separate integration of eqs. (3) and (4) is required to handle the numerical stiffness due to gas-phase reactions.

Numerical stiffness also occurs in the transient integration due to surface chemistry. To efficiently handle numerical stiffness, the routine DASPK, designed for large scale stiff DAE systems, performs the integrations [11].

The basic solution algorithm is to integrate the solid/surface equations (eqs. (5) to (7)) a finite amount forward in time, Δt, assuming that the axially varying gas-phase values are constant parameters. The code, upon reaching Δt, integrates eqs. (3) and (4) along the length of the channel keeping the solid/surface values (T_S, Z_k, Y_{kW}, and $\dot{s}_k$) fixed. The series of spatial and temporal integrations continue to some forward time (usually steady-state). This method of solution essentially lags the gas phase by the amount Δt during the time integration. For the calculations presented in this paper, Δt was set to $1/1000^{th}$ of the characteristic solid time scale, τ_S, based on the maximum calculated dT_S/dt in the domain at the previous timestep. That is $\Delta t = 0.001 \cdot \tau_S$ where $\tau_S = T_S \cdot [(dT_S/dt)_{max}]^{-1}$. The solution's dependence on Δt is discussed in the results.

Experiment

The experiments used a single horizontal cylinder (ID = 0.8 mm, OD = 1.0 mm) of 99.95% pure platinum. The experimental hardware is described in another paper [12]. The fuel is carbon monoxide in pure oxygen with ϕ ranging from 0.6 to 0.9 and an inlet velocity of 2 m/s.

The experiment begins by flowing a pre-mixed gas at room temperature through the tube which is also at room temperature. The flame from a butane lighter heats the outlet of the tube (for 5 to 10 sec) until it begins to glow dull orange (see fig. 1(b)). When the lighter is removed the glowing region propagates upstream along the channel at a slow speed (~mm/s). Figure 1 shows images of an ignition and propagation sequence. In this figure, image A shows the platinum tube and support fitting before the test. Figure 1(b) shows the ignition process with a gaseous flame from the lighter. Figure 1(b) also shows a gaseous CO flame coming from the tube outlet but it is not stable and extinguishes immediately after removing the lighter. Image C shows the tube midway through propagation while image D shows the flame stabilized near the tube inlet. The mechanism for flame stabilization is heat loss to the large fitting at the inlet.

Results and Discussion

Figure 2 shows the position of the leading edge of the propagating glowing region as a function of time for ϕ ranging from 0.6 to 0.9. In the experimental video analysis, the first frame after the removal of the lighter corresponds to 0 sec in the graph. The scatter in the initial location of the flame front is from the variability in manually placing and removing the

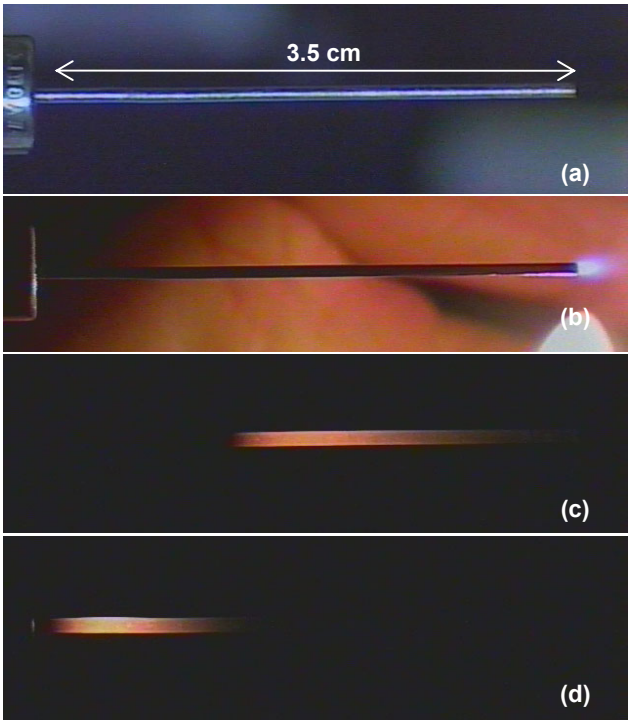

Figure 1.—Ignition and propagation sequence of a CO/O_2 (ϕ = 0.8) catalytic reaction along a platinum tube (0.8 mm ID, 1.0 mm OD). The inlet gas velocity is 2 m/s.

igniter. Model predictions of the leading edge of the propagation region are also in figure 2. For the model, the leading edge of the propagation zone is the location where the ratio of wall to bulk mass fraction of the fuel or oxidizer first decrease below 0.5 (i.e., a good indication where catalytic reactions are rapid and become mass-transfer limited). For the model data, zero time is when the ignition source turns off (i.e., 2 or 3 sec after the computation starts). The leading edge of the propagation zone advances prior to the removal of heat generation in the solid for the 3 sec ignition. The model did not ignite after 2 sec for ϕ = 0.8 and 0.9.

Figure 3 shows the propagation velocity for both the experiment and model. The velocity is the slope of a linear curve fit of the data from 2.5 to 1 cm in figure 2. This region limits the influence of the ignition transient and tube inlet. The experimental velocities are the average values from each propagation test (7 to 8 per condition). The error bars shown in the figure represent one standard deviation for the tests at a given ϕ.

The data in figure 3 shows that the model currently over predicts the average propagation velocity by roughly 40%. Some possible reasons for this discrepancy include inaccuracies in internal and external heat-transfer correlations and kinetic data. The qualitative features of the model results, however, match the experimental data. The data suggest that a longer ignition time affects the onset of propagation of the reaction zone. For instance, the ϕ = 0.6 and 0.7 experimental data agree more closely with the actual position of the catalytic flame for the 2 sec ignition time compared with the 3 sec time.

In the 3 sec ignition time (red lines in fig. 3), the catalytic flame is ahead of the experiment in all but 1 case during the $\phi = 0.9$ testing. Once the ignition transient subsides, the data show that the propagation velocity is not very sensitive to ϕ (with about a 10% increase in propagation velocity from $\phi =$ 0.6 to 0.9).

Finally, the solutions dependence on Δt is shown in figure 3. Again, Δt is the fraction of the fastest time scale (τ_S) in the domain computed from the solid energy equation at the previous timestep. Figure 3 shows a small dependence in propagation velocity (about 1.5% decrease) from $\Delta t = 0.01 \cdot \tau_S$ to $\Delta t = 0.001 \cdot \tau_S$ but at approximately 10 times the computational effort. A computation at $\Delta t = 0.0005 \cdot \tau_S$ showed no further change in propagation velocity to 3 significant digits.

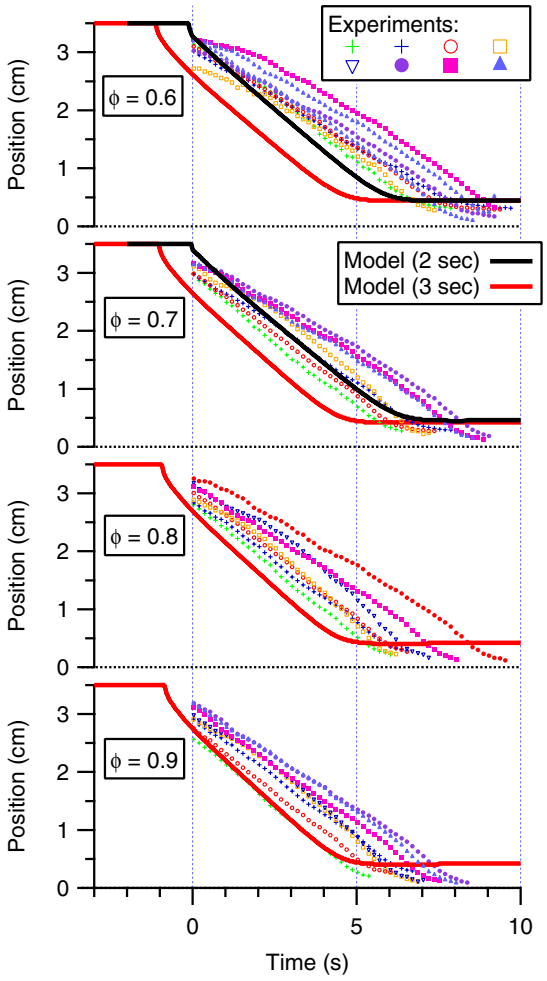

Figure 2.—Leading edge of catalytic flame position versus time for both the model (2 ignition durations) and multiple test runs. The variability in the experimental data is attributed to a non-uniform ignition.

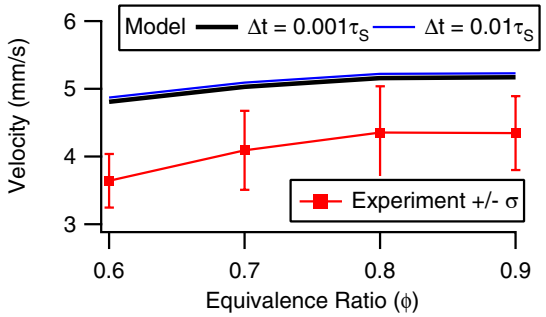

Figure 3.—Propagation velocity versus equivalence ratio for the experiment and model.

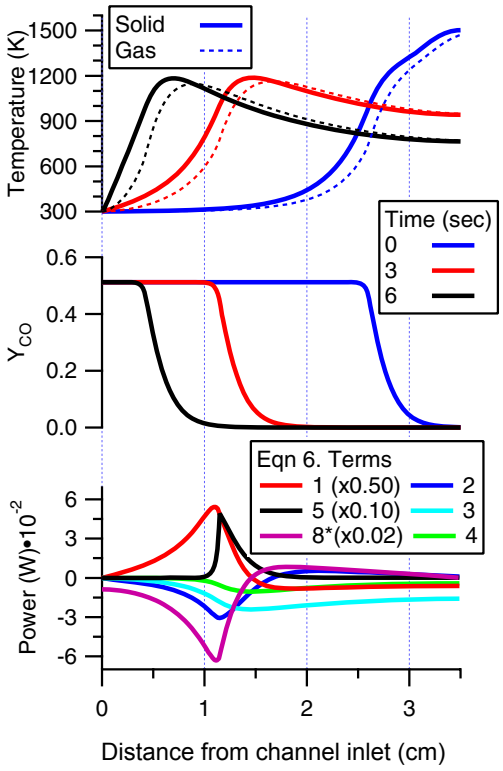

Figure 4.—Model predictions of the solid temperature profiles (top graph) and mass fraction of CO (middle graph) along the channel for 3 times corresponding to $\phi = 0.6$ (3 sec ignition time). In this graph, time = 0 corresponds to igniter turn-off. The bottom graph shows the profiles of various terms from the solid energy equation (eq.)6)) at 3 sec after the removal of the igniter.

The adiabatic flame temperatures for the mixtures used in this study exceed 2900 K. Figure 4 shows the solid and gas temperature profiles (top graph) at three different times during the computation for the $\phi = 0.6$ case with a 3 sec ignition. This figure also shows (middle graph) the mass fraction profiles which indicate almost complete conversion of the CO. This is true for the other equivalence ratios as well. Thus, almost all of

the reactants chemical energy is being released but is transferred elsewhere reducing local temperatures well below adiabatic.

The bottom graph in figure 4 shows the profiles of the various terms from the solid energy equation (eq. (6)) for each control volume used in the calculation. Each term (except 8*) is multiplied by the width of the local control volume so that the units are watts. The data in this graph corresponds to 3 sec after ignition turns off. At this point, the catalytic reaction front is still propagating towards the inlet of the channel. Terms 1 (solid heat-up), 5 (heat generated due to surface adsorption/desorption reactions), and 8^* (axial conduction) are multiplied by the constants shown in the graph for display purposes. In figure 4, the curve labeled 8^* shows the conductive heat transfer at the face of each axial control volume ($-kA_S \cdot dT_S/dx$) which also has units of watts. This term is quite large compared to its derivative which appears in eq. (6)—this latter term may mislead one to interpret that axial heat conduction is not important in this problem. Upstream axial conduction, however, is the largest form of heat transfer in the solid. During propagation, the energy goes to preheating the upstream solid (term 1). At steady-state (not-shown), the flame anchors near the inlet and the majority of the heat is conducted to the upstream heat-sink. Of the remaining terms (for both propagation and steady-state), the largest term (2) is convective heat transfer to the internal gas. At the moment shown in the bottom of figure 4, the solid heats the gas from the inlet to approximately 1.65 cm. After this point, the gas now heats the downstream solid which has cooled due to external heat losses. The majority of the external heat loss is to natural convection (term 3) and, to a lesser extent, radiation (term 4).

For an adiabatic or near-adiabatic channel such as in the interior of a catalytic monolith, the temperatures can approach that of an adiabatic flame. Thus, a monolith requires much lower equivalence ratios to keep within material limits. Future studies are planned with adiabatic conditions to investigate light-off characteristics for these conditions. Also, ceramic substrate materials with very different thermo physical properties will be investigated.

Conclusions

We have demonstrated both numerically and experimentally that a catalytic reaction can be initiated at the outlet of a small platinum tube which propagates upstream along the channel. These results (i.e., a catalytic channel with external heat loss) represent a conservative demonstration of the feasibility of back-end ignition for a catalytic metal monolith for which the interior channels approach adiabatic conditions. The experimental data presented show that the catalytic flame propagation velocity along the channel ranges from 3 to 4 mm/s for a 0.8 mm ID/1.0 mm OD pure platinum tube with CO in pure O_2 flowing at 2 m/s. The model over predicts the propagation velocities by about 40%. The propagation velocity is only a weak function of inlet equivalence ratio with about a 10% increase in propagation velocity from $\phi = 0.6$ to 0.9. For these non-adiabatic conditions, the model shows that the solid and interior gas temperatures are well below the mixture adiabatic temperatures despite near complete conversion of the CO. The majority of the heat is conducted upstream via axial conduction. The heat goes mostly to preheating the solid (during propagation) and internal gas with the remainder lost to external natural convection and radiation. At steady-state, the majority of heat loss is to the upstream heat-sink.

References

[1] R.A. Dalla Betta, *Catal. Today* **35** (1997) 129–135.

[2] P. Forzatti, G. Groppi, *Catal. Today* **54** (1999) 165–180.

[3] J.S. T'ien, *Combust. Sci. Technol.* **26** (1981) 65–75.

[4] F.P. Incropera, D.P. Dewitt, *Fundamentals of Heat and Mass Transfer 3rd ed.,* John Wiley and Sons, New York, 1990, pp. 355–356.

[5] S.W. Churchill, H.H.S. Chu, *Int. J. Heat Mass Tran.* **18** (1975) 1049–1053.

[6] P.M. Struk, D.L. Dietrich, B.P. Mellish, F.J. Miller, and J. S. T'ien, "Transient Catalytic Combustor Model with Detailed Gas and Surface Chemistry," *Proc. 4th Joint Meeting U.S. Sections Combust. Inst.*, March 20–23, 2005.

[7] S.G. Davis, A. V. Joshi, H. Wang and F. Egolfopoulos, *P. Combust. Inst.* **30** (2005) 1283-1292.

[8] S.G. Davis, A.V. Joshi, H. Wang and F. Egolfopoulos, http://ae-www.usc.edu/research/combustion/Combustion Kinetics/model_release.html (cited 17 March 2006).

[9] O. Deutschmann, R. Schmidt, F. Behrendt and J. Warnatz, *P. Combust. Inst.* **26** (1996) 1747–1754.

[10] O. Deutschmann, R. Schmidt, F. Behrendt and J. Warnatz, http://www.detchem.com/mechanisms/ (cited 17 March 2006).

[11] K.E. Brennan, S.L. Campbell and L.R. Petzold., *The Numerical Solution of Initial Value Problems in Differential-Algebraic Equations,* SIAM Classics Series, 1996, Chap. 5.

[12] F.J. Miller, B.P. Mellish, P.M. Struk, D.L. Dietrich, and J.S. T'ien, "Propagating Flames and Acoustic Instabilities in Tubular Microcombustors," *Proc. Central States Section Combust. Inst.*, May 21–23, 2006.

REPORT DOCUMENTATION PAGE		Form Approved OMB No. 0704-0188

1. REPORT DATE *(DD-MM-YYYY)*	2. REPORT TYPE	3. DATES COVERED *(From - To)*
18-06-2007	Technical Memorandum	

4. TITLE AND SUBTITLE
Catalytic Ignition and Upstream Reaction Propagation in a Platinum Tube

5a. CONTRACT NUMBER

5b. GRANT NUMBER
NNC04AA29A

5c. PROGRAM ELEMENT NUMBER

6. AUTHOR(S)
Struk, P., M.; Dietrich, D., L.; Mellish, B., P.; Miller, F., J.; T'ien, J., S.

5d. PROJECT NUMBER

5e. TASK NUMBER

5f. WORK UNIT NUMBER
WBS 519205.02.02

7. PERFORMING ORGANIZATION NAME(S) AND ADDRESS(ES)
National Aeronautics and Space Administration
John H. Glenn Research Center at Lewis Field
Cleveland, Ohio 44135-3191

8. PERFORMING ORGANIZATION REPORT NUMBER
E-15934

9. SPONSORING/MONITORING AGENCY NAME(S) AND ADDRESS(ES)
National Aeronautics and Space Administration
Washington, DC 20546-0001

10. SPONSORING/MONITORS ACRONYM(S)
NASA

11. SPONSORING/MONITORING REPORT NUMBER
NASA/TM-2007-214801

12. DISTRIBUTION/AVAILABILITY STATEMENT
Unclassified-Unlimited
Subject Categories: 25, 34, and 37
Available electronically at http://gltrs.grc.nasa.gov
This publication is available from the NASA Center for AeroSpace Information, 301-621-0390

13. SUPPLEMENTARY NOTES

14. ABSTRACT
A challenge for catalytic combustion in monolithic reactors at elevated temperatures is the start-up or "light-off" from a cold initial condition. In this work, we demonstrate a concept called "back-end" catalytic ignition that potentially can be utilized in the light-off of catalytic monoliths. An external downstream flame or Joule heating raises the temperature of a small portion of the catalyst near the outlet initiating a localized catalytic reaction that propagates upstream heating the entire channel. This work uses a transient numerical model to demonstrate "back-end" ignition within a single channel which can characterize the overall performance of a monolith. The paper presents comparisons to an experiment using a single non-adiabatic channel but the concept can be extended to the adiabatic monolith case. In the model, the time scales associated with solid heat-up are typically several orders of magnitude larger than the gas-phase and chemical kinetic time-scales. Therefore, the model assumes a quasi-steady gas-phase with respect to a transient solid. The gas phase is one-dimensional. Appropriate correlations, however, account for heat and mass transfer in a direction perpendicular to the flow. The thermally-thin solid includes axial conduction. The gas phase, however, does not include axial conduction due to the high Peclet number flows. The model includes both detailed gas-phase and catalytic surface reactions. The experiment utilizes a pure platinum circular channel oriented horizontally though which a CO/O_2 mixture (equivalence ratios ranging from 0.6 to 0.9) flows at 2 m/s.

15. SUBJECT TERMS
Catalysis; Platinum; Surface reactions; Heat transfer; Energy conversion

16. SECURITY CLASSIFICATION OF:			17. LIMITATION OF ABSTRACT	18. NUMBER OF PAGES	19a. NAME OF RESPONSIBLE PERSON
a. REPORT	b. ABSTRACT	c. THIS PAGE			Peter M. Struk
U	U	U		12	19b. TELEPHONE NUMBER *(include area code)* 216-433-5948